

Vortex line in superfluid ^4He : A variational Monte Carlo calculation

S. A. Vitiello

*Laboratory of Atomic and Solid State Physics, Cornell University, Ithaca, New York 14853
and Dipartimento di Fisica, Università degli Studi, Via Celoria 16, 20133 Milano, Italy*

L. Reatto

*Instituto Nazionale Fisica della Materia and Dipartimento di Fisica, Università degli Studi,
Via Celoria 16, 20133 Milano, Italy*

G. V. Chester and M. H. Kalos

Laboratory of Atomic and Solid State Physics, Cornell University, Ithaca, New York 14853

(Received 11 January 1996)

We present a Monte Carlo investigation of a vortex line in superfluid ^4He in a cylindrical container. We compute the excitation energy and the density profile for two different trial functions. The first is the standard Onsager-Feynman form for an excited vortex state. This gives a singular velocity on the axis of the vortex and a hollow core. In our second approach, a shadow wave function, is used to model the vortex state through the auxiliary, or shadow variables. As a consequence, the vorticity is distributed over a finite region and the density does not vanish at the vortex axis. This second wave function gives a substantially lower energy than the wave function of the Onsager-Feynman form. [S0163-1829(96)06625-8]

I. INTRODUCTION

Since the first observations^{1,2} of quantized vortices in superfluid helium four a large body of experimental and theoretical work has been carried out. Much of this work has been recently reviewed in detail.^{3,4} The basic picture of a quantized vortex has not changed over a period of 30 years. An isolated vortex, for example a vortex line or ring, consists of an extended irrotational flow field which can be accurately described by classical inviscid equations of motion. This flow field has as its source a core region where the vorticity is concentrated. The simplest and most important manifestation of the quantization of the flow is that the circulation is quantized in units of h/m . Here h is Planck's constant and m is the mass of the helium atom. Remarkably there is no evidence for the existence of quantized vortices with more than one unit of circulation. In spite of the large amount of experimental and theoretical work we still have no clear picture of the structure of the core region of a quantum vortex.^{3,4} Two simple, but basic, questions need to be answered. First how is the vorticity distributed in the core? Second how does the density of the fluid vary in the core? The experimental data on quantized rings have been analyzed using several different classical models of the core.³⁻⁵ For all of these models we find that the length scale associated with the core is about 1 Å. This result tells us that if we are to make progress in answering these two questions we will have to construct a microscopic theory. There have been a number of attempts⁶⁻¹² to construct a theory of the structure of a three-dimensional quantized vortex. However none of these deal satisfactorily with the strong interparticle correlations which exist on a length scale of a few angstroms. The purpose of this paper is to present the first results of a theory which deals directly with these correlations.

In this paper we will present two different calculations of

the core structure. Both are variational calculations based on model excited states for a single quantum vortex. First we will take as our model state the well-known Onsager-Feynman^{9,10} state. We will evaluate the expectation values by Monte Carlo integration; apart from statistical sampling errors our results are exact for this model. As we have pointed out, this state leads to a hollow core with a singular source for the vorticity. Our numerical work allows us to determine accurately the size of the core of the vortex. We present this calculation both to clarify the structure of this simple model and to develop our Monte Carlo techniques for this problem.

Our second calculation is more ambitious and much more difficult to carry out. It uses a model vortex state constructed from a shadow wave function. These wave functions were first introduced to provide an unbiased description of the crystalline phase of helium four.^{13,14} They have been shown to provide an accurate description of the homogeneous fluid and solid phases,¹⁵ the excitation spectrum,¹⁶ and the fluid-solid interface.¹⁷ The main advantage of this type of wave function is that it provides great flexibility in modeling states of liquid and solid helium. Shortly after the introduction of shadow wave functions it was shown¹⁸ that a vortex state could be constructed that had both nonzero density and distributed vorticity in the core region. We present a Monte Carlo calculation of the energy and other properties of this new vortex state. We find a lower energy as compared with that of the Onsager-Feynman state. In addition we find a nonzero density throughout the core region. For reasons which we will shortly describe this Monte Carlo calculation is very difficult to carry out with the desired accuracy. We believe that we have overcome this difficulty by the application of sufficient computing power. Our results are however somewhat limited. In our discussion we will suggest alternative strategies which we hope will enable us to perform this

kind of Monte Carlo calculation in a much more efficient fashion.

Very recently the core structure of a vortex in two-dimensional ^4He has been investigated by Ortiz and Ceperley.¹⁹ In addition to the Onsager-Feynman form for the phase, they have allowed for backflow effects in the phase. This is an alternative way to have delocalized vorticity. In fact it is known¹⁸ that introducing a phase factor in the shadow variables is a way to represent backflow effects in the real variables.

II. MODEL WAVE FUNCTIONS

In this work we consider two model wave functions to describe a vortex line in a system of N helium atoms. The first has the well-known Onsager-Feynman form,^{9,10} or a form closely related to it as discussed in Sec. IV:

$$\Psi_F(R) = e^{i\phi} \prod_{j=1}^N f(\rho_j) \Psi_0(R), \quad (1)$$

where Ψ_0 is the ground state for the system and $R \equiv \{\mathbf{r}_j | j=1, \dots, N\}$ where \mathbf{r}_j are the coordinates of the atoms. We use cylindrical coordinates (ρ, ϕ, z) with the z axis along the vortex line. The phase factor $\phi = \sum_{j=1}^N \phi_j$ depends on the angular variables ϕ_j of the particles and the function f on their radial distance ρ_j from the vortex axis. The function $f(\rho)$ controls the density as a function of the radial distance. The wave function Ψ_F describes a quantized vortex line with circulation $\kappa = h/m$, with localized vorticity on the vortex axis and a purely tangential velocity field $v_\phi(r) = \hbar/m\rho$. Because of the divergence of v_ϕ at the vortex axis, the function $f(\rho)$ has to vanish as $\rho \rightarrow 0$. As a consequence the local density $n(\rho)$ vanishes as $f^2(\rho)$. To implement our Monte Carlo calculation we need to choose a functional form for f . Our form is

$$f(\rho) = 1 - e^{-(\rho/a)^2}, \quad (2)$$

where a is a variational parameter. This particular functional form gave the lowest vortex excitation energy in a previous calculation which used approximate integral equations¹¹ to compute the energy. For the ground state Ψ_0 we use a variational shadow wave function.¹³ This allows a direct comparison between results obtained with the function Ψ_F and the excited-state shadow wave function described below.

We compute the expectation value of the energy by standard Monte Carlo methods; and therefore we have to consider a finite number of particles. A simple choice is to restrict the N particles to be inside a cylinder of radius \mathcal{R} and height L , with the vortex axis at the center of the cylinder. On its lateral surface we assume rigid boundary condition, i.e., Ψ_0 vanishes when a particle is on this surface. In the z direction we impose periodic boundary conditions. In this way, our system is uniform in the direction of the vortex axis but it is inhomogeneous in the radial direction. There is another way to set up the simulation of a line vortex. This is to take a periodic array of line vortices with alternating signs. Their velocity fields will therefore cancel at large distances and the entire systems will be at rest. The fluid will be homogeneous except in the core regions. Such a system lends itself to a finite simulation with periodic boundary condi-

tions. We plan to carry out this type of simulation and compare the results with those of this paper.

The shadow wave function we use to describe this inhomogeneous system is

$$\Psi_0(R) = \psi(R) \int K(R, S) \psi_s(S) dS, \quad (3)$$

where $S \equiv \{\mathbf{s}_j | j=1, \dots, N\}$. Here \mathbf{s}_j is a shadow coordinate and $dS = ds_1 ds_2 \dots ds_N$. The functions ψ and ψ_s are both Jastrow functions multiplied by one-body terms

$$\psi(R) = \chi(R) \prod_{j<l} e^{-(1/2)u(r_{jl})} \quad (4a)$$

and

$$\psi_s(S) = \chi_s(S) \prod_{j<l} e^{-u_s(s_{jl})}, \quad (4b)$$

with $\chi(R) = \prod_{j=1}^N \tanh d(\mathcal{R}^2 - r_j^2)$, where d is a variational parameter. We use the same form for $\chi_s(S)$, but a different length parameter d_s . This form for $\chi(R)$ guarantees that Ψ_0 vanishes at the wall of the cylinder. Equation (4a) describes the correlations of the particles and Eq. (4b) describes the correlations of the shadow variables. The pseudopotentials u and u_s are of the McMillan form:

$$u(r_{jl}) = \left(\frac{b}{|\mathbf{r}_j - \mathbf{r}_l|} \right)^5 \quad (5a)$$

and

$$u_s(s_{jl}) = \left(\frac{b_s}{|\mathbf{s}_j - \mathbf{s}_l|} \right)^9, \quad (5b)$$

where b and b_s are variational parameters. The factor $K(R, S)$ couples the particles and the shadows through a product of Gaussians:

$$K(R, S) = \prod_j e^{-C|\mathbf{r}_j - \mathbf{s}_j|^2}, \quad (6)$$

and C is a variational parameter. Our wave function for the ground state of helium in a cylindrical container has five variational parameters, b , b_s , C , d , and d_s . Without the factors $\chi(R)$ and $\chi_s(S)$ in Eqs. (4a) and (4b), $\Psi_0(R)$ of Eq. (3) is the standard shadow wave function for homogeneous liquid ^4He .

As we discussed in the Introduction, we expect that the vorticity associated with a line vortex is delocalized around the axis with a related modification of the $1/\rho$ velocity field. It has already been shown¹⁸ that this is accomplished if the wave function of the vortex contains the phase factor expressed in terms of the shadow variables. Our second trial function for the vortex state is constructed employing this idea. It is given by the equation

$$\Psi_D(R) = \psi(R) \int e^{i\varphi} K(R, S) \psi_s(S) dS, \quad (7)$$

where $\varphi(S) = \sum_{j=1}^N \varphi_j$. The φ_j refer to the shadow coordinates. The other factors in Ψ_D are the same as in the ground state Ψ_0 .

The qualitative properties of this wave function have been described elsewhere.¹⁸ The wave function $\Psi_D(R)$ is an eigenstate of the total angular momentum operator with eigenvalue $N\hbar$. Hence it is a proper trial function for a vortex state. This wave function does not contain the modulating factors $f(\rho)$ that are present in $\Psi_F(R)$. In fact, such terms are not needed because the velocity field is finite everywhere. The velocity can be written in the form¹⁸

$$\mathbf{v}(\mathbf{r}) = \frac{\hbar}{2m} \int d\mathbf{s} \frac{1}{s} \frac{n(\mathbf{r},\mathbf{s})}{n(r)} \mathbf{u}_\phi. \quad (8)$$

In this equation $n(r)$ is the local density of particles and $n(\mathbf{r},\mathbf{s})$ is the pair distribution function for a particle with coordinate \mathbf{r} and one of its shadows with coordinate \mathbf{s} . The unit vector in the tangential direction is denoted by \mathbf{u}_ϕ . It is clear from (8) that the velocity field is smeared out over a distance of the order of the range of the function $n(r,s)$. This is controlled by the kernel K ; for a Gaussian the range is of order $C^{-1/2}$. The velocity field $\mathbf{v}(\mathbf{r})$ vanishes linearly with ρ when ρ is close to the vortex axis. The physical interpretation of the shadow wave function is that the shadow variables represent the quantum delocalization hole, of size $C^{-1/2}$, for each atom. This is also the minimum length over which any singularity will be smeared out.

The absence in $\Psi_D(R)$ of factors which modulate the density on the vortex axis means, in the first place, that this trial wave function has no variational parameters associated with the vortex. All the variational parameters are determined through the ground-state calculation. In the second place, the local density of particles is nonzero even at the axis of the vortex. So this function describes a vortex with delocalized vorticity and a core that is not hollow. This contrasts with the wave function $\Psi_F(R)$ that has localized vorticity and a hollow core.

III. COMPUTATION OF THE GROUND-STATE ENERGY AND DENSITY

We write the Hamiltonian of our system of helium atoms in the form

$$H = \sum_j (T_j + V_j). \quad (9)$$

T_j is the kinetic energy of the j th atom and V_j is the contribution of the potential energy associated with this atom. These quantities are given, respectively, by

$$T_j = -\frac{\hbar^2}{2m} \nabla_{\mathbf{r}_j}^2 \quad \text{and} \quad V_j = \frac{1}{2} \sum_{l(\neq j)} v(|\mathbf{r}_j - \mathbf{r}_l|). \quad (10)$$

For the interparticle potential $v(\mathbf{r}_{ij})$ we use the two-body HFDHE2 potential of Aziz *et al.*²⁰ Our calculations were performed for a system of 200 particles in a cylindrical container. The height of our simulation cell, $z_0 = 11.35 \text{ \AA}$, was the minimum for which finite-size effects along the z direction can be easily neglected. It corresponds to the edge of a cubical simulation cell of 32 atoms for bulk liquid helium. The radius $\mathcal{R} = 16.53 \text{ \AA}$ of the container was chosen so that the density in its central region is close to the liquid- ^4He

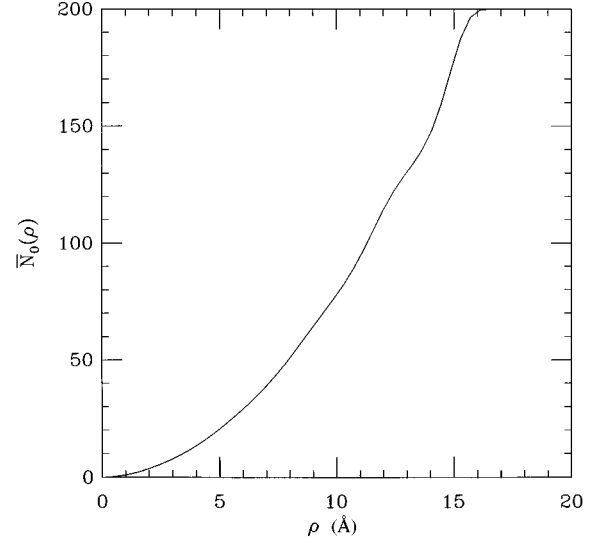


FIG. 1. The ground-state integrated density $\bar{\mathcal{N}}_0(\rho)$, Eq. (11), as a function of radial distance ρ . The cylinder has a radius of 16.5 \AA .

equilibrium density. With the boundary conditions that the wave function vanish on the cylindrical surface, the density will vanish there.

The first step in the calculation is to determine the ground-state energy. The expectation value of H is computed using configurations sampled with the Metropolis algorithm. The energy was minimized for the following set of parameters: $b = 1.13$, $b_s = 1.20$, $C = 4.0$, $d = 0.06$, and $d_s = 0.09$. Our system is inhomogeneous so it is important to have local probes of the properties of the system. We compute the local density $n(\rho)$ as a function of the radial distance ρ . The average number of particles $\bar{\mathcal{N}}_0(\rho)$ at a distance less or equal to ρ from the container's axis is then given by,

$$\bar{\mathcal{N}}_0(\rho) = z_0 \int_0^\rho n(\rho') d^2 \rho'. \quad (11)$$

In addition we estimate the following energy function:

$$\bar{\mathcal{E}}_0(\rho) = \left\langle \sum_{j=1}^N \theta(\rho - \rho_j) \frac{(T_j + V_j) \Xi(R,S)}{\Xi(R,S)} \right\rangle_0. \quad (12)$$

The symbol $\langle \rangle_0$ denotes an average in the space $\{R, S, S'\}$ of particles and shadows taken with respect to configurations sampled from $\Xi(R,S)\Xi(R,S')/Q_0$, where we have defined $\Xi(R,S) = \psi(R)K(R,S)\psi_s(S)$ as the product of $\psi(R)$ and the integrand of Eq. (3). S' represents the second set of shadow coordinates that come in when the wave function is squared. Q_0 is the normalization factor of Ψ_0 . The function $\theta(x)$ is the step function: $\theta(x) = 1$ if $x \geq 0$ and $\theta(x) = 0$ otherwise. $\bar{\mathcal{E}}_0(\rho)$ represents the contribution to the local energy of those particles whose distance is less or equal to ρ from the container's axis. Thus $\bar{\mathcal{E}}_0(\rho)/\bar{\mathcal{N}}_0(\rho)$ represents the energy per particle for such particles. When ρ is equal to the cylinder's radius \mathcal{R} , $\bar{\mathcal{E}}_0(\mathcal{R})$ is just the estimate of the total ground-state energy.

In Figs. 1 and 2 we show $\bar{\mathcal{N}}_0(\rho)$ and $\bar{\mathcal{E}}_0(\rho)$. In both graphs we clearly see the inhomogeneous nature of the system. The oscillations are produced by the boundary conditions at the cylindrical surface. However, when we plot the ratio

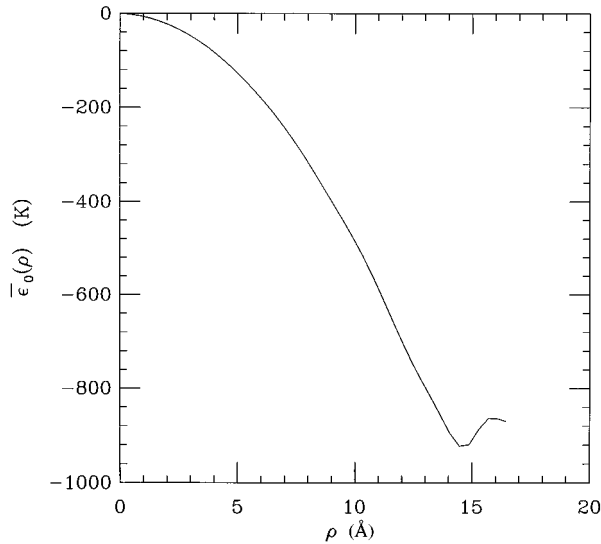


FIG. 2. The ground-state energy $\bar{\mathcal{E}}_0(\rho)$, Eq. (12) as a function of radial distance ρ .

$\bar{\mathcal{E}}_0(\rho)/\bar{\mathcal{N}}_0(\rho)$, Fig. 3, we see that these oscillations are largely removed in the interior of the cylinder. Moreover, the average energy per particle up to 8 Å is -6.25 K, this is very close to the energy per particle, -6.24 K, obtained with this shadow wave function for homogeneous liquid helium. This is an important feature of our simulation. In the ground state of our cylindrical container we have a reasonably homogeneous region in the interior of the cylinder, with an energy per particle close to that of bulk helium.

For large values of ρ , near the wall, $\bar{\mathcal{E}}(\rho)/\bar{\mathcal{N}}(\rho)$ has a sharp increase. At $\rho=\mathcal{R}$, the variational energy per particle of the system includes the contributions given by the surface of the fluid at the wall. In fact, we can estimate this surface energy ΔE as $[\bar{\mathcal{E}}_0(\mathcal{R})-NE_0]/2\pi\mathcal{R}z_0$, where E_0 is the average value of the energy in the inner region. We find $\Delta E=0.32$ K/Å². As expected, this is larger than the liquid-vacuum interface surface energy,²¹ which is about 0.27 K/Å².

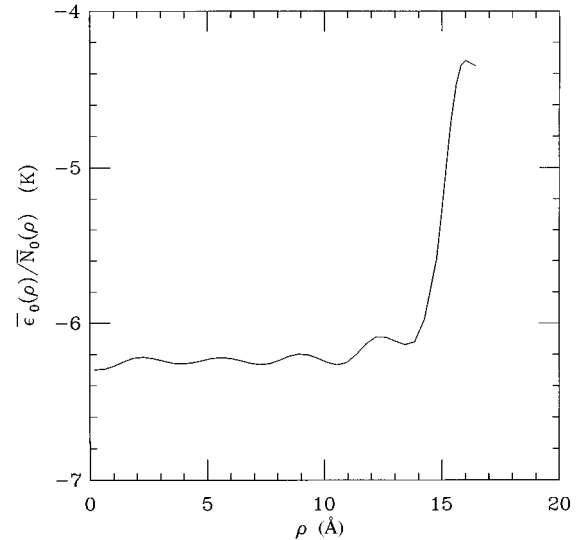


FIG. 3. The ratio of energy to integrated density for the ground state, $\bar{\mathcal{E}}_0(\rho)/\bar{\mathcal{N}}_0(\rho)$, as a function of radial distance ρ .

IV. RESULTS FOR THE VORTEX LINE

We now present our results for the system with a vortex line. First consider the Onsager-Feynman shadow wave function of Eq. (1). The excitation energy is obtained as the difference between the expectation values of H determined with the vortex wave function Ψ_F and with the ground state Ψ_0 . All evidence is that the size of the vortex core is very small, of order of a few Å. This fact makes the core contribution to the vortex energy small compared to that of the kinetic energy of the long-range potential flow. This last contribution is just equal to that of a vortex in a classical incompressible fluid. Thus it is important to consider not only the total excitation energy of the system, but to separate out the contribution coming from particles in the inner region of the container. In a way similar to what we have done in the previous section, we introduce the contribution to the vortex excitation energy per unit length due to particles up to a distance ρ from the vortex axis. For the Onsager-Feynman form (F) it is given by

$$\bar{\mathcal{E}}_F(\rho) = \frac{1}{z_0} \left\langle \sum_{j=1}^N \theta(\rho - \rho_j) \left[\frac{\hbar}{2m} \frac{1}{\rho_j^2} + \frac{(T_j + V_j)F(R)\Xi(R,S)}{F(R)\Xi(R,S)} \right] \right\rangle_F - \frac{1}{z_0} \bar{\mathcal{E}}_0(\rho). \quad (13)$$

The symbol $\langle \rangle_F$ stands for an average taken with configurations sampled from

$$F^2(R)\Xi(R,S)\Xi(R,S')/Q, \quad (14)$$

where $F(R)=\prod_{i=1}^N f(\rho_i)$ and Q is the appropriate normalization factor. At $\rho=\mathcal{R}$, the first term in Eq. (13) is the total energy for the excited state per unit length of the vortex. The first term in the inner brackets is the contribution to the kinetic energy due to the phase factor of Ψ_F . The expression between brackets in Eq. (13) can be derived by taking into

account the Hermitian properties of H and the equivalence of the two sets of shadow variables. Two independent runs, one that samples configurations from $|\Psi_F|^2$ and the other from $|\Psi_0|^2$, are needed to estimate the vortex excitation energy $\bar{\mathcal{E}}_F(\rho)$.

We have also performed the computation with a wave function in which the shadow variables also have the same modulating factor $F(S)$ as the particles. In this case the average in Eq. (13) is taken with respect the weight

$$F^2(R)F(S)\Xi(R,S)F(S')\Xi(R,S')/Q,$$

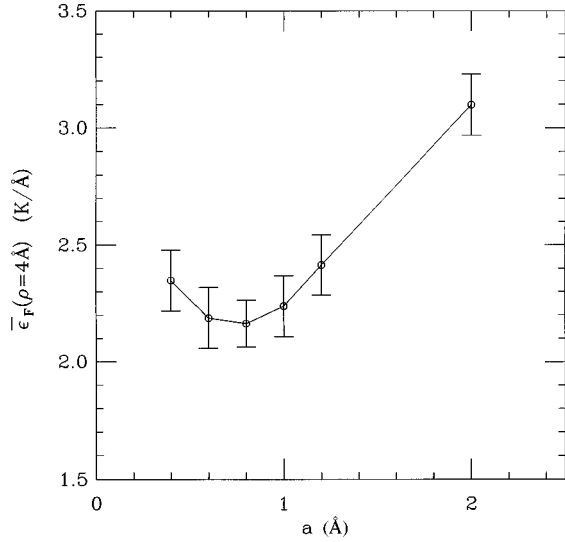


FIG. 4. The energy $\bar{\mathcal{E}}_F(\rho)$, evaluated for $\rho=4 \text{ \AA}$, as a function of the variational parameter a .

we also call this an Onsager-Feynman wave function because the phase factor is identical to that of Eq. (1). The only difference is in the modulating real part of the wave function which is not simply a product of one-body terms as in (1) but higher-order terms are implicitly contained via integration over the shadow variables. We have found that this wave function in which the same Gaussian hole is present both in the particle and in the shadow variables gives a slightly lower energy. All the results we quote below for the Onsager-Feynman vortex refer to this form, i.e., to the weight (14).

As we already mentioned, the vortex function Ψ_F depends on an additional variational parameter a , which is present in the function $f(\rho)$, Eq. (2). The dependence of the excitation energy $\bar{\mathcal{E}}_F(\rho)$ on a is very similar for different values of ρ . In Fig. 4 we show results obtained at $\rho=4 \text{ \AA}$. The minimum excitation energy is for $a=0.8 \text{ \AA}$. We present in Fig. 5 the vortex excitation energy per unit length, $\bar{\mathcal{E}}_F(\rho)$, as a function of the radial distance ρ . The excitation energy varies from about 1 K/\AA for $\rho=3 \text{ \AA}$ to approximately 3 K/\AA for the full system. Figure 6 tells us that when $\rho=3 \text{ \AA}$ the density profile of the fluid is close to its unperturbed value. Classically, the vortex energy has a logarithmic dependence on ρ . For a vortex line with circulation $\kappa=h/m$, this classical energy per unit length is

$$\epsilon_{\text{cl}}(\rho) = \frac{\pi \hbar^2 n}{m} \left(\ln \frac{\rho}{\beta} - \delta \right), \quad (15)$$

where n is the average number density of the fluid, β is the radius of the vortex core, and δ is a number of order unity that depends on the model of the core. We find that our result for the energy of the quantum vortex is well represented by a similar functional form. A fit over the range $2\text{--}12 \text{ \AA}$ gives the result

$$\bar{\mathcal{E}}_F(\rho) = 0.83 \left(\ln \frac{\rho}{0.8} + 0.73 \right) \text{ K/\AA}, \quad (16)$$

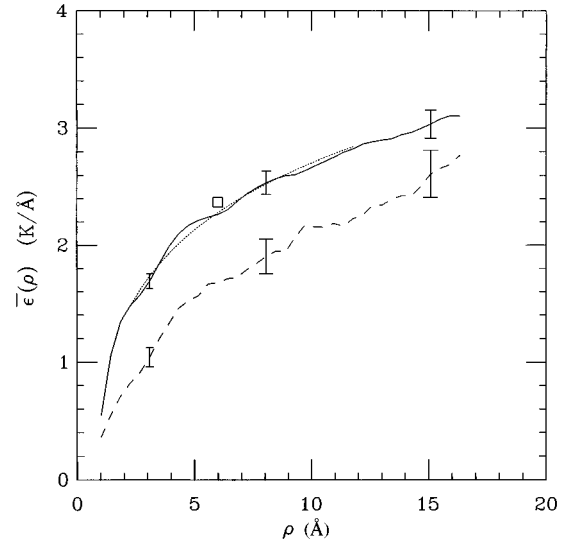


FIG. 5. The energy of a vortex per unit length $\bar{\mathcal{E}}(\rho)$. The continuous curve shows $\bar{\mathcal{E}}_F(\rho)$, Eq. (13). The dashed curve shows $\bar{\mathcal{E}}_D(\rho)$, Eq. (17). The dots show the energy given by Eq. (15). The open square is the value of the energy computed by Chester *et al.* (Ref. 11).

where ρ is in \AA and we have used the value $a=0.8 \text{ \AA}$ as a length parameter in the logarithmic function. This function is also shown in Fig. 5. Notice that the value of the constant term in Eq. (15) is not uniquely determined but depends on the choice of the length parameter in the logarithm. The function $\bar{\mathcal{E}}_F(\rho)$ displays some slight oscillations in its variation with ρ . They are clearly related to the modulation of the density profile shown in Fig. 1.

An earlier calculation of the energy¹¹ for the Onsager-Feynman wave function used the Percus-Yevick and HNC approximate integral equations to evaluate the energy expectation value. The calculations were performed at a radial dis-

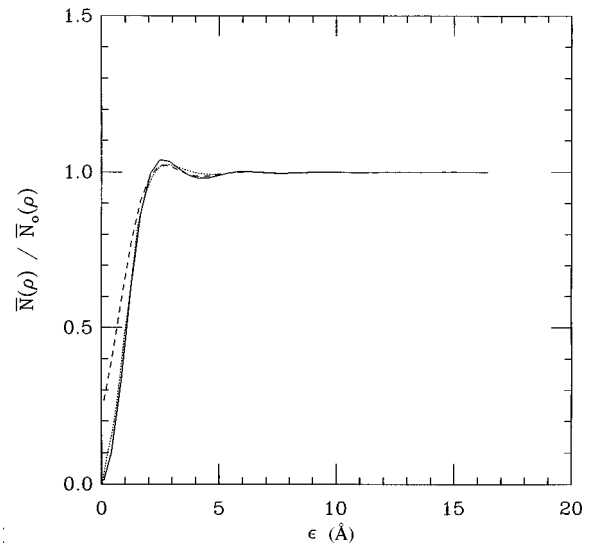


FIG. 6. The ratio of average number of particles for the system with a vortex to average number of particles for the system in the ground state. The continuous curve shows the ratio $\bar{\mathcal{N}}_F(\rho)/\bar{\mathcal{N}}_0(\rho)$, the dashed curve shows $\bar{\mathcal{N}}_D(\rho)/\bar{\mathcal{N}}_0(\rho)$. The dots show the profile calculated by Chester *et al.* (Ref. 11).

tance equal to 6 Å and the energy was found to be 2.37 K/Å. This result is shown in Fig. 5 and it is very close to the energy 2.25 K/Å that we find at this radial distance. More recently Dalfovo¹² has computed the vortex energy on the basis of density functional theory. He finds an energy 3 K/Å for $\rho=17$ Å, a value similar to but slightly above our result at $\rho=\mathcal{R}=16.53$ Å.

The density profile computed using this trial function is shown in Fig. 6. It shows clearly the vanishing density at the axis and the fluctuations introduced by the presence of the hole at the vortex core. Above approximately 9 Å this density profile agrees with that of the ground state. The density reaches half the value at equilibrium at $\rho=0.9$ Å; and has two clear maxima due to the presence of the vortex. The other maxima are due to the layering produced by the container's wall. In the previous computations^{11,12} a similar behavior was found close to the vortex core, but the oscillations had a significantly smaller amplitude.

We now discuss our results for the shadow wave function with delocalized vorticity; Ψ_D given by Eq. (7). The simulations with this function are much more difficult to perform than those for Ψ_F . The vortex signature in the square of the Onsager-Feynman wave function $|\Psi_F|^2$ is just due to the real $F(R)$ and $F(S)$ factors. The phase factor only gives rise to the centrifugal $1/\rho^2$ term in the energy expression. On the contrary, with Ψ_D the phase factors do not cancel each other and give rise to large fluctuations of the integrand when a shadow is close to the vortex axis. In order to obtain reasonable statistics for the energy as a function of ρ we have performed a run of 60×10^6 Monte Carlo sweeps. This is a factor 30 longer than the runs performed with the Onsager-Feynman function.

The contribution to the vortex excitation energy due to particles within a distance ρ from the vortex axis can now be written in the form

$$\bar{\mathcal{E}}_D(\rho) = \frac{1}{z_0} \frac{\langle e^{-i(\varphi-\varphi')} \sum_{j=1}^N \theta(\rho-\rho_j) [(T_j + V_j) \Xi(R,S)/\Xi(R,S)] \rangle_0}{\langle e^{-i(\varphi-\varphi')} \rangle_0} - \frac{1}{z_0} \bar{\mathcal{E}}(\rho) \quad (17)$$

where the meaning of the symbols are the same as in Eq. (13), φ and φ' , are the sum of the angular variables of the shadows S and S' , respectively. The symbol $\langle \rangle_0$ stands for the average with respect to Ψ_0 . The denominator in Eq. (16) is the normalization constant for the function Ψ_D .

The behavior of $\bar{\mathcal{E}}_D(\rho)$ as a function of ρ is similar to that of the Onsager-Feynman wave function as can be seen from Fig. 5. However, the energy is on the average about 0.6 K/Å lower than that found for the Onsager-Feynman wave function. The difference is roughly constant for all ρ greater than 2 Å. This wave function, with delocalized vorticity, gives the lowest excitation energy for a vortex line in liquid ⁴He obtained so far. This is remarkable because this wave function has no additional variational parameters to describe the core of the vortex. If we fit $\bar{\mathcal{E}}_D(\rho)$ with the form given by Eq. (14) we find $\delta=-0.03$ when we take $\beta=0.8$ Å. This choice of β , allows a direct comparison with the energy, Eq. (16), of the Onsager-Feynman wave function. Since, outside the core region, the contribution to the excitation energy is essentially kinetic, and is the same for both wave functions, the core energy contribution of the vortex with delocalized vorticity must be smaller than that described by the Onsager-Feynman function.

The density profile obtained using Ψ_D is presented in Fig. 6. There is again a depletion of the density at the cylinder axis. However, the density is now nonzero at the vortex axis. The depletion of particles in the core region is significantly reduced compared with the hollow core of the Onsager-Feynman wave function. For instance the density reaches half the equilibrium value at $\rho=0.6$ Å, compared with 0.9 Å in the other case. The average number of particles within a distance of 1 Å from the vortex axis is 0.5 for Ψ_F compared with 0.7 for Ψ_D ; a 30% increase. Examining the amplitude of the first maximum of the density profile, Fig. 6, we see

that the amplitude obtained with the trial function with delocalized vorticity is significantly smaller than the one determined with the Onsager-Feynman wave function. This means that the vortex described by Ψ_D represents a smaller density perturbation of the homogeneous ground state and this presumably is the origin of the lower excitation energy.

V. CONCLUSION

We have presented the first study of a vortex excitation in superfluid ⁴He in three dimensions using Monte Carlo simulations. Our results for the Onsager-Feynman form of the wave function confirm the results of Chester *et al.*¹¹ based on an integral equation method. The vortex excitation energies from these two computations are very similar. However one should keep in mind the differences between the two calculations. In our simulation we have a finite cylindrical system in the direction transverse to the vortex axis; the system is inhomogeneous even in the ground state. In the earlier computation the vortex line was in bulk liquid. Here we have to assume an explicit, and therefore approximate, form for the ground state; the present choice has been a shadow wave function. The integral equation method requires only the ground-state pair-correlation function, which was taken from experiment. On the other hand, the integral equation introduces additional approximations whereas the Monte Carlo method gives exact results within statistical fluctuations for an approximate trial wave function.

The singularity of the vorticity field derived from the Onsager-Feynman wave function at the vortex axis is rather artificial and it is gratifying that we find a significantly smaller vortex excitation energy with a wave function that has delocalized vorticity. Here, the representation of interparticle correlations via the shadow variables has a funda-

mental role because the flow field is induced via these shadow variables. In this way, the vortex singularity is smeared out over the average distance between a particle and its shadow, a distance of order 1 \AA . Once again the present calculation shows that the shadow representation is very useful in introducing multiparticle correlations. The lowering of the vortex excitation energy with the wave function with delocalized vorticity comes from the region within a radius of about 5 \AA around the vortex axis, the region where the local density differs appreciably from the ground state. This lowering is quite significant because it amounts to about 30%. Outside this region the energy is essentially due to the classical flow field and so there is no essential difference between the two wave functions.

There is no other theoretical computation for a vortex with delocalized vorticity in three-dimensional ^4He to compare with our results. However, it is instructive to make some comparisons with the results¹⁹ for ^4He in two dimensions (2D). Both computations give a lowering of the vortex energy when the vorticity is distributed rather than singular. In our computation this lowering of the core energy seems to be substantially larger than in the 2D case but this might be due in part to the rather large statistical uncertainty of the two computations. Both computations give a nonzero but strongly reduced density in the core. The size of this core is of the same order of magnitude, 1 \AA , but it is somewhat larger in the 2D case. We do not know if these differences are due to the different dimensionality or to the different form of the wave functions. In case of roton excitations it is known¹⁶ that introducing the phase in the shadow variables gives an excitation energy which is substantially lower than that of a Feynman-Cohen explicit backflow computation.

Of particular significance in superfluid ^4He are vortex ring excitations. This requires a much more complex form of the wave function. However for large vortex rings we can proceed to use our results for a line vortex. As mentioned above, the present calculation shows that the contribution to the excitation energy of the quantum vortex is essentially equal to the classical one for distances larger than about 5 \AA from the vortex axis. In a bulk liquid sample, let us consider a vortex ring of radius R with a toroidal region centered at the circle of radius R and with a radius b_0 . It is around this toroidal region that we consider the flow field. We can approximate the contribution to the excitation energy coming from the region as $2\pi R\varepsilon(b_0)$, where $\varepsilon(b_0)$ is the excitation per unit length of a vortex line up to a distance b_0 . This quantity $\varepsilon(b_0)$ is given by either $\bar{\mathcal{E}}_D(b_0)$ or $\bar{\mathcal{E}}_F(b_0)$. For the outer region of the toroid we approximate the excitation energy with that of a classical vortex ring of circular cross section. This corresponds to the energy of a vortex ring of radius R and a hollow core of size b_0 , i.e., $E(R, b_0) = (1/2)\kappa^2[\ln(8R/b_0) - 2]$ where the circulation has the quantum value $\kappa = h/m$. The excitation energy of a vortex ring with this approximation is

$$E_{\text{ring}}(R) = \frac{h^2}{2m} nR \left[\ln \frac{8R}{b_0} - \alpha(b_0) \right], \quad (18)$$

where $\alpha(b)$ is given by

$$\alpha(b_0) = 2 - \frac{4\pi m}{h^2 n} \varepsilon(b_0). \quad (19)$$

If we take $b_0 = 5 \text{ \AA}$ and for $\varepsilon(b_0)$ the energy $\mathcal{E}_D(5 \text{ \AA}) = 1.53 \text{ K/\AA}$, corresponding to the vortex with delocalized vorticity, we get $\alpha(5 \text{ \AA}) = 0.16$. If we use $\mathcal{E}_F(5 \text{ \AA}) = 2.17 \text{ K/\AA}$, corresponding to Onsager-Feynman case, we get $\alpha(5 \text{ \AA}) = -0.61$. Notice that as long as the dependence of $\varepsilon(b_0)$ on b_0 is well represented by Eq. (14), the energy of the ring, Eq. (18), does not depend on the choice of b_0 . The length b_0 . The length b_0 in Eq. (18) should not be confused with the core diameter or with the healing length, here it is just the distance where we join the outer with the inner region.

There is no direct measurement of the core energy of a vortex line in ^4He , however we can get some information about it from results obtain for vortex rings. The Rayfield and Reif results² have been interpreted by Glabertson and Donnelly³ in terms of an energy of a vortex ring of radius R_0 that can be written in the form

$$E_{\text{ring}}(R_0) = \frac{h^2}{2m} nR_0 \ln \frac{8R_0}{l} \quad (20)$$

with $l = 5.98 \text{ \AA}$ at equilibrium density. Our approximate theoretical expression (18) for the energy can be written in the form of Eq. (20). For the vortex with delocalized vorticity the parameter l is then $l_D = 5.87 \text{ \AA}$, in very good agreement with experiment. For the Onsager-Feynman form, l is the $l_F = 2.72 \text{ \AA}$. The close agreement between experiment and theory when a vortex with delocalized vorticity is used is very encouraging and supports the notion that the vortex core has a complex structure. In order to check that the agreement is not fortuitous it will be important to perform a similar comparison at higher densities.

As a by-product of the present computation we get an estimation of the surface energy of ^4He at a hard wall, $\Delta E = 0.32 \text{ K/\AA}^2$.

Our study represents the first exploration of the core structure of a three-dimensional vortex line in ^4He . This study can be pursued usefully in different directions. We have studied a wave function with delocalized vorticity which has no variational parameters for the vortex. By introducing in Ψ_D a real one-body term, one could modulate the density in the core region, both up or down compared with what we have now, and see if this lowers the core energy. In the second place, the smearing of the vortex singularity takes place over a distance that is determined by the parameter C in the Gaussian that couples particles to shadows. In the present calculation the value of C is left unchanged from its optimum value in the ground state. A more flexible wave function for the vortex might have a C that depends on the distance of a particle from the vortex axis or on the value of the local density.

ACKNOWLEDGMENTS

We want to thank David Ceperley for useful discussions. This work (L.R. and S.A.V.) has been supported in part by Consiglio Nazionale delle Ricerca under Progetto Finalizzato "Sistemi Informatici e Calcolo Parallelo." This work was also supported by the Condensed Matter Theory Program of

the National Science Foundation under Grant No. DMR-9200469, and was conducted using the resources of the Cornell Theory Center, which receives major funding from the National Science Foundation, and New York State. Addi-

tional funding comes from the Advanced Research Projects Agency, the National Institutes of Health, IBM Corporation, and other members of the center's Corporate Research Institute.

-
- ¹W. F. Viven, Proc R. Soc A **260**, 218 (1961).
²G. W. Rayfield and F. Reif, Phys. Rev. **136**, A1194 (1964).
³W. I. Glaberson and R. J. Donnelly, in *Progress in Low Temperature Physics*, edited by D. Brewer (North-Holland, Amsterdam, 1986), Vol. IX.
⁴R. J. Donnelly, *Quantized Vortices in He II* (Cambridge University Press, Cambridge, 1991).
⁵M. Steingart and W. I. Glaberson, Phys. Rev. Lett. **14**, 585 (1965).
⁶V. L. Ginzburg and L. D. Landau, Zh. Eksp. Teor. Fiz **20**, 1064 (1950); V. L. Ginzburg and L. P. Pitaevskii, Sov. Phys. JETP **7**, 858 (1958).
⁷A. L. Fetter, Phys. Rev. **138**, A429 (1965).
⁸E. P. Gross, Nuovo Cimento **20**, 454 (1961).
⁹L. Onsager, Nuovo Cimento Suppl. **6**, 249 (1949).
¹⁰R. P. Feynman, in *Progress in Low Temperature Physics*, edited by C. Gorter (North-Holland, Amsterdam, 1955), Vol. I.
¹¹G. V. Chester, R. Metz, and L. Reatto, Phys. Rev. **175**, 275 (1968).
¹²F. Dalfovo, J. Low Temp. Phys. **89**, 453 (1992).
¹³S. A. Vitiello, K. Runge, and M. H. Kalos, Phys. Rev. Lett. **60**, 1970 (1988).
¹⁴S. A. Vitiello, K. Runge, G. V. Chester, and M. H. Kalos, Phys. Rev. B **42**, 228 (1990).
¹⁵T. McFarland, S. A. Vitiello, L. Reatto, G. V. Chester, and M. H. Kalos, Phys. Rev. B **50**, 13 577 (1994).
¹⁶D. M. Galli, L. Reatto, and S. A. Vitiello, J. Low Temp. Phys. **101**, 755 (1995).
¹⁷F. Pederiva, A. Ferranti, S. Fantoni, and L. Reatto, Phys. Rev. Lett. **72**, 2589 (1994).
¹⁸S. A. Vitiello, L. Reatto, and M. H. Kalos, in *Condensed Matter Theories*, edited by V. C. Aguilera-Navarro (Plenum, New York, 1989).
¹⁹G. Ortiz and D. M. Ceperley, Phys. Rev. Lett. **75**, 4624 (1995).
²⁰R. A. Aziz, V. P. S. Nain, J. S. Carley, W. G. Taylor, and G. T. McConville, J. Chem. Phys. **70**, 4330 (1979).
²¹H. M. Guo, D. O. Edwards, R. E. Sarwinski, and J. T. Tough, Phys. Rev. Lett. **27**, 1259 (1971).